Rayleigh-Taylor Instability Experiments Examining Feedthrough Growth in an Incompressible, Convergent Geometry

S. T. Weir, E. A. Chandler, and B. T. Goodwin

Lawrence Livermore National Laboratory, University of California, P.O. Box 808, Livermore, California 94551

(Received 29 September 1997)

We have performed Rayleigh-Taylor instability and feedthrough growth experiments in a 2D cylindrically convergent geometry by imploding gelatin cylinders with high-pressure gases. Instability growth was seeded by fabricating sinusoidal undulations on the outer surfaces of the cylinders, which were then observed during implosion with high-speed framing cameras. These experiments are the first to study feedthrough perturbation growth in an incompressible, convergent geometry. We compare the results to small-amplitude perturbation analysis and to a recent radiation-drive feedthrough experiment. [S0031-9007(98)05987-0]

PACS numbers: 47.40.–x, 47.20.Bp, 47.20.Ma

The study of hydrodynamic instabilities in a convergent geometry is critical for understanding important features of inertial confinement fusion (ICF) experiments [1,2], supernova core collapses [3], and underwater explosions. In all of these phenomena, a lighter fluid accelerates a heavier fluid, which results in a Rayleigh-Taylor (RT) interfacial instability [4]. In the case of ICF experiments, a RT instability develops at the ablation interface where the high-pressure plasma pushes against the denser capsule shell. It is widely recognized that small nonuniformities in either the capsule surface or the drive illumination can seed the growth of RT instability modes. In the case of supernova core collapses, the apparent large-scale mixing suggested by observations of the supernova explosion SN 1987A has been attributed to RT instability growth [5,6]. For all of these examples, convergence plays an important role since it expands or compresses perturbation scales and alters the RT growth characteristics.

In ICF experiments, another factor that must be considered is "thin wall" effects, which can result in the appearance of perturbations on the inner surface of an imploding, spherical shell due to the feedthrough of perturbations from the outer, RT unstable surface. These inner surface perturbations are highly undesirable since they are believed to limit ICF capsule performance [2,7]. Again, convergence plays an important role since, as the capsule implodes, perturbation length scales change and the capsule shell thickens, thus affecting how the outer perturbations couple to and influence the inner surface perturbations.

Because of experimental difficulties in accurately controlling and diagnosing perturbations in a convergent geometry, most RT experiments have been planar geometry experiments, and relatively few experiments have been performed using convergent geometries [8]. We present here the results of a 2D, convergent geometry Rayleigh-Taylor experiment featuring precise control of initial perturbations and high-resolution images of the RT and feedthrough growth. Experiments of this type provide valuable data on RT and feedthrough growth in the inviscid, incompressible, large Atwood number limit.

In our Rayleigh-Taylor experiments, we studied instability growth modes on transparent gelatin cylinders imploded with high-pressure gases, a technique originally developed by Meshkov *et al.* [9]. The experimental apparatus is shown in Fig. 1. A cast cylinder of low-strength gelatin was sandwiched between transparent plates of Plexiglas and borosilicate glass in a hermetically sealed chamber. The gelatin cylinder consisted of a 6% concentration of gelatin (Kind & Knox Company; 225 Bloom gelatin) with water, and was gelled at 7 °C for at least 12 hours to form a low-strength elastic solid. The cylinder had an outer diameter of 11 cm and an inner diameter of 8 cm for a radial thickness ΔR of 1.5 cm. The axial thickness was 1 cm. The measured shear modulus was 0.07 bar and the Poisson's ratio was 0.5. By machining sinusoidal undulations on the Plexiglas molding parts used to cast the gelatin, we were able to fabricate precise perturbations on the outer surface of the cylinder to seed RT growth modes of interest. In this way, we fabricated a cylinder with a mode-6 perturbation having an amplitude of 1 mm. The outer surface was thus described by

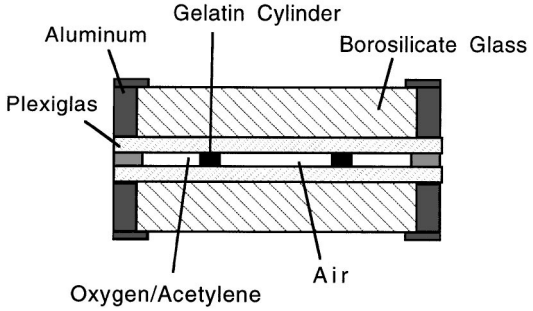

FIG. 1. Schematic diagram of the containment fixture. A 6% gelatin cylinder is sandwiched between two Plexiglas and borosilicate glass plates. The gas cavity surrounding the gelatin cylinder is filled with an equimolar mixture of oxygen and acetylene, while the gas cavity inside the cylinder is filled with air. High-pressure driving gas is created when the oxygen-acetylene mixture is detonated by 122 exploding bridge wires. High-speed framing cameras record axial images of the cylinder collapse.

0031-9007/98/80(17)/3763(4)$15.00

$R(\theta) = R_0 + A\sin(m_\theta\theta)$, where $R(\theta)$ is the outer radius as a function of azimuthal angle θ, R_0 (= 5.5 cm) is the unperturbed outer radius, A (= 1 mm) is the amplitude, and m_θ (= 6) is the mode number. Based on the surface roughness of the Plexiglas molding parts, we estimate gelatin surface roughness to be less than 10 μm, which is much less than the imposed perturbation amplitude of 1 mm. Prior to the experiment, the annulus outside the cylinder was filled with an equimolar mixture of oxygen and acetylene, while the inside of the gelatin cylinder was filled with air at 1 atm. A xenon flash lamp was used to backlight the cylinder for the 1.5 msec duration of the experiment. The entire implosion history of the cylinder was recorded by a high-speed framing camera (Cordin, Mod 6) running at 9 μsec/frame with a record length of 164 frames.

Instability growth occurs when the oxygen-acetylene gas mixture is detonated, and the cylinder implodes. To ensure a highly symmetric implosion, 122 exploding bridge wires (EBW's) were mounted inside the containment apparatus on a ring surrounding the oxygen-acetylene and were simultaneously burst with a high-voltage capacitor bank. Perturbations due to shock interactions between adjacent EBW's were negligible. The Chapman-Jouguet detonation front pressure of an equimolar oxygen-acetylene gas mixture is 45 atm (0.0045 GPa), which results in an initial inward radial acceleration of 8.8×10^6 cm/sec^2 at the outer surface. Since the pressure is much lower than the bulk modulus of water (= 2.2 GPa), the gelatin cylinder can be considered to be incompressible. Also, note that the elastic strength of the gelatin has a negligible effect on perturbation growth for modes which satisfy $k^2G/\rho\gamma^2 \ll 1$ [10], where k is the wave number, G is the gelatin shear modulus ($= 7 \times 10^4$ dyn/cm^2), ρ is the density (= 1 g/cm^3), and γ is the perturbation growth rate ($\approx$2800 sec^{-1}). For a mode-6 perturbation, k is 1.09 cm^{-1}, and so $k^2G/\rho\gamma^2 = 0.01 \ll 1$. Therefore, the elastic strength has very little influence on the growth rate of the imposed mode for the mode-6 experiment to be discussed. Finally, the initial perturbation amplitude of $A = 1$ mm is small compared to the amplitude threshold of $\approx 0.1\lambda$ (= 5.8 mm), where nonlinear effects such as mode coupling and harmonic growth become significant.

Figure 2 shows a sequence of framing camera images from this experiment. Several interesting features should be noted. As the cylinder implodes and the outer surface becomes RT unstable, a turbulent mix layer of detonation product gases and gelatin starts to propagate through the cylinder (dark region of the outer surface). This growth is seeded by surface roughness at the length scale of the most unstable growth mode, which is close to 0.18 mm, the cutoff wavelength for surface tension stabilization. In addition to the mix layer, instability growth also occurs at the imposed mode-6 wavelength, and this will be the focus of the rest of this paper. The mode-6 perturbation amplitude on the outer surface initially grows exponentially at a rate of $\gamma = 2800$ sec^{-1}, in good agreement with the classical growth rate of $\sqrt{kg} = 3100$ sec^{-1} for an inviscid, incompressible fluid. The resulting flow creates a mode-6 feedthrough perturbation on the inner surface, as seen in Figs. 2(a) and 2(b). The amplitude of the feedthrough perturbation grows to approximately 0.5 mm at 550 μsec [Fig. 2(b)], while the perturbation on the outer surface has grown from 1 to 2.43 mm. Thus, the observed attenuation is 0.21 (= 0.5/2.43), in very good agreement with the predicted attenuation factor of $\exp(-k\Delta R) = 0.19$ from planar feedthrough theory [11], where k and ΔR are evaluated at $t = 0$. At later times, the amplitude of the feedthrough perturbation amplitude stagnates, decreases to zero [Fig. 2(c)], and, finally, at 756 μsec [Fig. 2(d)] the amplitude becomes negative; i.e., the feedthrough perturbation has reversed its phase. A plot of the feedthrough amplitude is shown in Fig. 3. Also shown is the predicted feedthrough from planar theory. The agreement is very good up to about 550 μsec, but then planar theory completely fails to model the subsequent feedthrough inversion behavior.

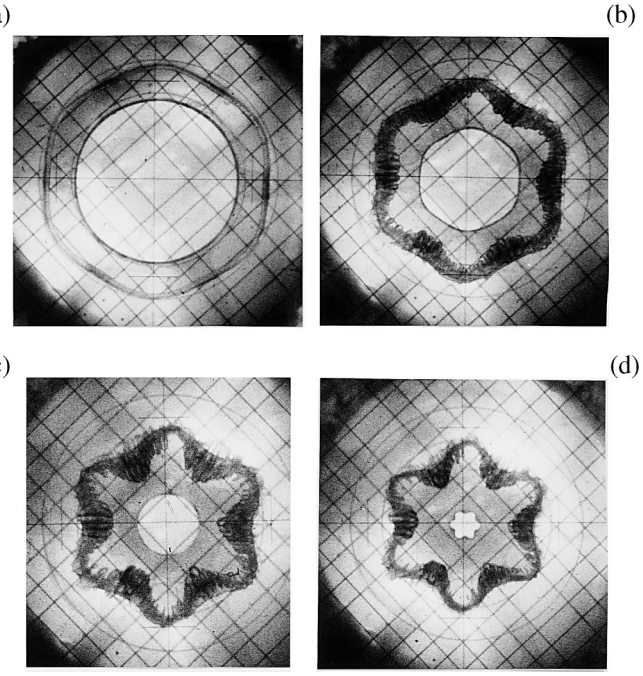

FIG. 2. Implosion of a mode-6 cylinder with an initial perturbation amplitude of $A = 1$ mm. (a) $t = 225$ μsec; (b) $t = 549$ μsec; (c) $t = 675$ μsec; (d) $t = 756$ μsec.

The cylinder acceleration history based on a Lagrangian analysis calculation of the cylinder motion [12] is shown in Fig. 4. The Lagrangian analysis assumed an elastic, incompressible cylinder, which is radially imploded by the adiabatic expansion of high-pressure gas in the annulus surrounding the cylinder. Potential energy terms included the energy of the expanding gas surrounding the cylinder, the compression of the gas inside the cylinder, and the elastic potential energy of the cylinder itself. Lagrange's equation was then solved numerically and a very good agreement between the observed and calculated cylinder

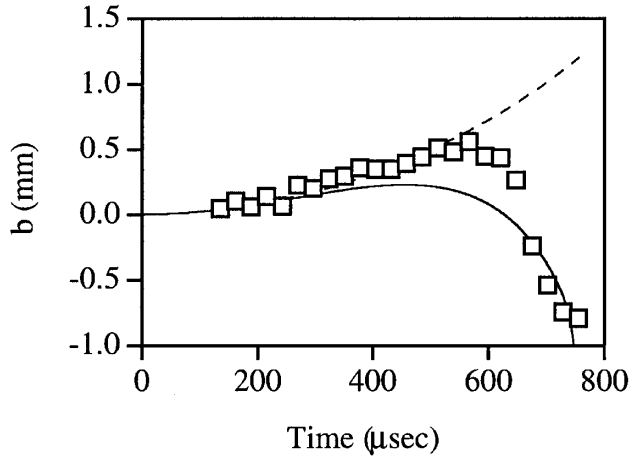

FIG. 3. Feedthrough perturbation amplitude $b(t)$ vs time. Experimental data points are indicated by small squares. The dashed line is the prediction based on planar feedthrough theory [11]. The solid line is the result of the small-amplitude analysis described in the text.

collapses was obtained when P_0, the initial pressure of the gas outside the cylinder, was set to 16.5 atm. From Fig. 4 one sees that, for the first 550 μsec, both the outer and inner surfaces are accelerating inward, so the outer surface is RT unstable and the inner surface is stable. From 550 to 740 μsec, the accelerations for the outer and inner surfaces are directed in opposite directions, with the outer surface accelerating outwards, and the inner surface continuing to accelerate inwards, so both interfaces are RT stable at this stage. Finally, at 740 μsec, the inner surface starts to accelerate outwards, and this interface becomes RT unstable. This sequence of acceleration stages is primarily determined by the time-varying geometry of the gelatin cylinder itself, and is relatively insensitive to the detonation pressure or to the equations of state used to model the gases.

Since small amplitude analysis has been applied to the study of perturbation growth on spherical shells [13,14], it is straightforward to derive the perturbation growth equations for cylindrical rings [12]. Here, we will outline

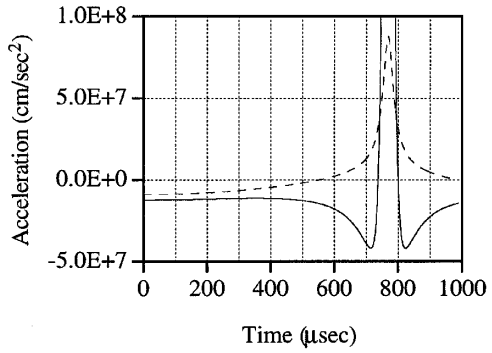

FIG. 4. Radial acceleration vs time. The solid line is the acceleration history at the inner surface of the cylinder and the dashed line is the acceleration history at the outer surface of the cylinder. Negative accelerations correspond to inward accelerations, and positive to outward accelerations.

the approach used. A more detailed description will be published [12]. We used the fact that the pressure must be continuous across the outer and inner surfaces of the ring, and then applied Euler's equation to obtain two linear, coupled, 2nd order differential equations in $a(t)$ and $b(t)$, the amplitudes of the outer and inner perturbations, respectively. The differential equations can be cast in the form [12]

$$a''(t) = G_{11}a'(t) + G_{12}a(t) + G_{13}b'(t) + G_{14}b(t), \tag{1}$$

$$b''(t) = G_{21}b'(t) + G_{22}b(t) + G_{23}a'(t) + G_{24}a(t), \tag{2}$$

where the G_{ij}'s are time-dependent functions of the outer cylinder radius $r_0(t)$, the inner radius $r_i(t)$, and the mode number m_θ. The initial conditions are $a(0) = A$, $a'(0) = 0$, $b(0) = 0$, and $b'(0) = 0$. At $t = 0$, G_{12} and G_{24} are

$$G_{12} = \frac{gm_\theta}{R_0}\left(\frac{1 + \Psi^{2m_\theta}}{1 - \Psi^{2m_\theta}}\right);$$

$$G_{24} = \frac{2gm_\theta}{R_0}\left(\frac{\Psi^{m_\theta - 2}}{1 - \Psi^{2m_\theta}}\right),$$

where g is the inward acceleration at the outer surface of the cylinder, R_0 is the initial outer radius, R_i is the initial inner radius, and $\Psi = R_i/R_0$ (= 0.727). Note that, at $t = 0$, the outer perturbation is growing exponentially at a rate governed by G_{12}. In addition, a positive feedthrough perturbation is starting to grow at a rate governed by the cross-coupling function G_{24}. To determine the full time evolution of $a(t)$ and $b(t)$, Eqs. (1) and (2) were numerically integrated using the $r_0(t)$ and $r_i(t)$ determined from the Lagrangian analysis. As seen in Fig. 3, the calculated feedthrough $b(t)$ describes the observed feedthrough behavior much better than does planar feedthrough theory.

Examination of the numerical values of the G_{ij} coefficients at various times provides some insight into the evolution of the feedthrough growth, which can be roughly broken into three stages.

(i) *A strong-coupling stage ($t < 450$ μsec).*—In this stage, there is significant coupling between the functions $a(t)$ and $b(t)$ of Eqs. (1) and (2) (i.e., G_{14} and G_{24} are relatively large), and the RT growth of the outer perturbation strongly drives the growth of the feedthrough perturbation. During this stage, the feedthrough amplitude $b(t)$ scales very well with $a(t)\exp(-k\Delta R)$, in agreement with planar feedthrough theory.

(ii) *A decoupling stage ($450 < t < 740$ μsec).*—During this stage, the functions $a(t)$ and $b(t)$ of Eqs. (1) and (2) become weakly coupled to each other (coefficients G_{12} and G_{22} become at least an order of magnitude larger than the other coefficients) and to a very good approximation the equations describe two nearly free and independent harmonic oscillators. This decoupling is a result of two influences. The outer surface acceleration becomes positive (i.e., outward) as seen in Fig. 4, and so

the outer surface becomes RT stable. In addition, the radial thickness ΔR increases due to increasing convergence as the cylinder collapses. The feedthrough perturbation which developed during stage (i) now starts to undergo a nearly free oscillation, resulting in the observed phase inversion.

(iii) *Deceleration stage.*—During this stage, the inner surface starts to decelerate and becomes RT unstable, resulting in rapid exponential growth of any existing feedthrough perturbations.

It is interesting to compare the feedthrough development in our incompressible experiment with a recent compressible feedthrough experiment involving a radiation-driven cylindrical implosion [15]. In the radiation-drive experiment, an initial strong-coupling stage was observed in which the growth of the feedthrough perturbation at a marker layer was consistent with the $\exp(-k\Delta R)$ attenuation factor. At a later stage when the marker layer interface became RT stable, the growth of the perturbation was shown to be consistent with Bell-Plesset [16] growth, which is a geometrical convergence effect. In contrast to the radiation-driven experiment, we find that the Bell-Plesset effect plays a very minor role in the feedthrough growth of our incompressible experiment, except just before the deceleration stage. This difference appears to be attributable to the fact that, in the radiation-drive experiment, the outer perturbations are carried by an ablation front which propagates through the cylinder during the experiment, thus reducing the effective ΔR and ensuring significant perturbation coupling throughout the experiment. Thus, $\exp(-k\Delta R)$ scaling holds until convergence eventually forces the appearance of Bell-Plesset growth. In our incompressible experiments, however, there is no ablation front, and ΔR increases due to convergence. In addition, the incompressible nature of our experiments together with the convergent geometry causes the outer surface acceleration to drop significantly during the implosion. As a result, a perturbation decoupling stage occurs about halfway through the implosion, which leads to the observed phase inversion. Finally, note that, in a radiation-driven experiment, both the strong coupling stage and the Bell-Plesset stage preserve the phase of the feedthrough perturbation, so feedthrough phase inversions such as we observed are not normally expected to occur.

In summary, we have performed Rayleigh-Taylor instability feedthrough experiments in an incompressible, convergent geometry, and have observed the growth of the feedthrough perturbation. The observed feedthrough growth characteristics are in better agreement with the behavior predicted by our small-amplitude analysis than with planar theory. During the initial strong-coupling stage, the feedthrough perturbations scale according to the $\exp(-k\Delta R)$ attenuation factor. At a later stage, the feedthrough perturbation becomes decoupled from the outer perturbation and starts to undergo nearly free harmonic oscillations which, in our experiment, results in a feedthrough phase inversion.

Rayleigh-Taylor experiments with gelatin cylinders and high-pressure gas drives offer the ability to perform well-controlled and well-characterized convergent geometry experiments in the inviscid, incompressible, large Atwood number limit. This experimental technique offers the potential of performing quantitative, high-resolution experiments to study not only feedthrough growth, but also other important related topics such as mode-mode coupling and turbulent mix development in convergent geometries.

We thank the technicians B. Gray, D. Anderson, A. Hernandez, D. Burns, C. Clements, and M. Moss for their invaluable work on the experiments. We also acknowledge valuable discussions with B. Remington, K. Mikaelian, R. Benjamin, R. Lee, P. Urtiew, and J. Chase. This research was supported by B-Division at Lawrence Livermore National Laboratory under the auspices of the U.S. Department of Energy under Contract No. W-7405-ENG-48.

[1] E. M. Campbell, Laser Part. Beams **9**, 209 (1991).
[2] J. D. Kilkenny, S. G. Glendinning, S. W. Haan, B. A. Hammel, J. D. Lindl, D. Munro, B. A. Remington, S. V. Weber, J. P. Knauer, and C. P. Verdon, Phys. Plasmas **1**, 1379 (1994).
[3] L. Smarr, J. R. Wilson, R. T. Barton, and R. L. Bowers, Astrophys. J. **246**, 515 (1981).
[4] G. Taylor, Proc. R. Soc. London A **201**, 192 (1950); Lord Rayleigh, Proc. London Math. Soc. **14**, 170 (1883).
[5] I. Hachisu, T. Matsuda, K. Nomoto, and T. Shigeyama, Astrophys. J. **390**, 230 (1992).
[6] E. Müller, B. Fryxell, and D. Arnett, Astron. Astrophys. **251**, 505 (1991).
[7] J. D. Lindl and W. C. Mead, Phys. Rev. Lett. **34**, 1273 (1975).
[8] W. W. Hsing and N. M. Hoffman, Phys. Rev. Lett. **78**, 3876 (1997); H. Nishimura, H. Takabe, K. Mima, F. Hattori, H. Hasegawa, H. Azechi, M. Nakai, K. Kondo, T. Norimatsu, Y. Izawa, C. Yamanaka, and S. Nakai, Phys. Fluids **31**, 2875 (1988); J. S. Wark, J. D. Kilkenny, A. J. Cole, M. H. Key, and P. T. Rumsby, Appl. Phys. Lett. **48**, 969 (1986); M. A. Sweeney and F. C. Perry, J. Appl. Phys. **52**, 4487 (1981).
[9] E. E. Meshkov, N. V. Nevmershitsky, V. G. Rogachev, and I. G. Zhidov, in *Proceedings of the 4th International Workshop on the Physics of Compressible Turbulent Mixing, Cambridge, England, 1993* (Cambridge University, Cambridge, England, 1993), p. 578.
[10] S. M. Bakhrakh *et al.,* University of California Report No. UCRL-CR-126710.
[11] G. Taylor, Proc. R. Soc. London A **201**, 192 (1950).
[12] S. T. Weir, E. A. Chandler, and B. T. Goodwin (to be published).
[13] M. S. Plesset, J. Appl. Phys. **25**, 96 (1954).
[14] K. O. Mikaelian, Phys. Rev. A **42**, 3400 (1990).
[15] W. W. Hsing and N. M. Hoffman, Phys. Rev. Lett. **78**, 3876 (1997).
[16] G. I. Bell, Los Alamos Scientific Laboratory Report No. LA1321, 1951; M. S. Plesset, J. Appl. Phys. **25**, 96 (1954).